**SPE 123988**

# Successful Carbonate Well Log Facies Prediction Using an Artificial Neural Network Method: Wafra Maastrichtian Reservoir, Partitioned Neutral Zone (PNZ), Saudi Arabia and Kuwait

Hong Tang, SPE, Niall Toomey, and W. Scott Meddaugh, SPE, Chevron Energy Technology Company



This paper was prepared for presentation at the 2009 SPE Annual Technical Conference and Exhibition held in New Orleans, Louisiana, USA, 4–7 October 2009.



## Abstract

The Maastrichtian (Upper Cretaceous) reservoir is one of five prolific oil reservoirs in the giant Wafra oil field. The Maastrichtian oil production is largely from subtidal dolomites at an average depth of 2500 feet. Carbonate deposition occurred on a very gently dipping, shallow, arid, and restricted ramp setting that transitioned between normal marine conditions to restricted lagoonal environments. The average porosity of the reservoir interval is about 15%, although productive zones have porosity values up to 30-40%. The average permeability of the reservoir interval is about 30 md. Individual core plugs have measured permeability up to 1200 mD.

The currently available core data for the Maastrichtian is limited to six wells, five of which are essentially along the axis of the reservoir. As a result, the use of this core data set for stratigraphic and depositional interpretation is somewhat limited. This study was undertaken to determine: (1) if facies could be successfully predicted (classified) from well log data and (2) if the predicted facies could be used to extend the stratigraphic and depositional interpretation to the flanks of the reservoir.

Efforts to predict facies from well logs in carbonate reservoirs is difficult due to the complex carbonate facies structures, strong diagenetic overprint, and challenging log analysis due in part to the presence of vugs and fractures. In the study, a workflow including (1) core description preprocessing (2) log and core data clean-up, and (3) probabilistic neural network (PNN) facies analysis was used to accurately predict facies from log data. First, the core descriptions were digitized and the number of facies reduced from twenty to six (mudstone, packstone, mud-rich packstone, grain-rich packstone, grainstone, and floatstone). Next, the log data for the cored wells were normalized and ”cleaned” by removing intervals with incomplete data, evidence of significant vugs (or fractures in very limited cases), poor well bore conditions, or acoustic log or resistivity log spikes.

For validation purpose, training sets were randomly selected from two cored wells. Hold-off data were used to validate prediction ability. The log data used for facies prediction include seven curves - GR, SP, DT, NPHI, RHOB, PE, and RT. GR spectrum logs, which are generally better lithological logs than GR were available for only a few wells; therefore, GR spectrum logs were not used in this study.

After evaluation of a variety of statistical approaches, a probabilistic neural network PNN-based approach was used to predict facies from well log data. PNN was selected as a tool because it has the capability to delineate complex nonlinear relationships between facies and log data. PNN was shown to outperform multivariate statistic algorithms and in this study gave good prediction accuracy (above 70%). The prediction uncertainty was quantified by two probabilistic logs - discriminant ability and overall confidence. These probabilistic logs can be used to evaluate the prediction uncertainty during interpretation. Lithofacies were predicted for 15 key wells in the Wafra Maastrichtian reservoir and effectively used to extend the understanding of the Maastrichtian stratigraphy, depositional setting, and facies distribution.

## Introduction

The Cretaceous-age Maastrichtian reservoir at Wafra Field in the PNZ has complex depositional and post-depositional history (Dull et al, 2006). The reservoir description and stratigraphic framework study of Dull et al (2006) was limited as most of the available cored wells were along the strike of the structure. Consequently, there is considerable uncertainty about the vertical and lateral distribution of depositional facies. The quality of the available 3D seismic volume precluded its use to assist in quantitative definition of the stratigraphic architecture of the Maastrichtian reservoir. This study was undertaken to determine if facies could be predicted from the wireline logs and if the predicted facies data could be used to improve our understanding of the vertical and lateral distribution of depositional facies. Multivariate statistics methods were compared and ultimately, a probabilistic neural network (PNN) model was selected and optimized using multiple well logs as input. The predicted facies were cross validated using hold off data as well as by blind well test.

Log data are widely used in clastic reservoirs to predict facies in un-cored well intervals. However, due to the complexity of carbonate depositional facies, strong diagenetic overprint, and often challenging logging conditions due in part to vugs and fractures, it is difficult to classify facies from log data using traditional cutoff methods. The methods that have been used to classify carbonate facies using wireline logs can be generalized in two major categories:

1. Empirical methods which include using the Archie equation or rock fabric equation, to classify facies (Asquith (1985); Holtz and Major (2004); Lucia (2005))
2. "Statistical" approaches such as multivariate statistics, fuzzy logic and neural network methods that characterize the complex nonlinear relationship of carbonate facies and wireline log parameters.

This study is focused on the statistical approaches.

Lim et al. (1997) used principle component analysis (PCA) and cluster analysis to classify facies from wireline logs with moderate success. Lee et al. (2004) and Mathisen et al. (2003) applied PCA, model based cluster analysis (MCA), and discriminant analysis to characterize electrofacies types and used non-parametric regression to predict permeability of a carbonate reservoir in West Texas. Lim and Kim (2004) reported using fuzzy logic and neural networks to delineate the non-linear relationship between the best related well logs and reservoir properties. Qi and Carr (2006) successfully used a back propagation neural network to predict carbonate facies. Statistical analysis and geological information were used to constrain their neural network modeling.

To improve the performance of neural networks, Wong et al. (1998) addressed important issues of improving neural network performances such as sample de-biasing, outlier removal, and log calibration. They successfully applied a neural network to predict permeability in a laminated shale/sandstone reservoir using a backward propagation neural net. In general, successful application of neural networks requires clear petrophysical and geological classification. Data pre-processing using various statistical methods, outlier removal, data normalization, and use of synthetic logs should improve neural net performance (Wong et al., 1998).

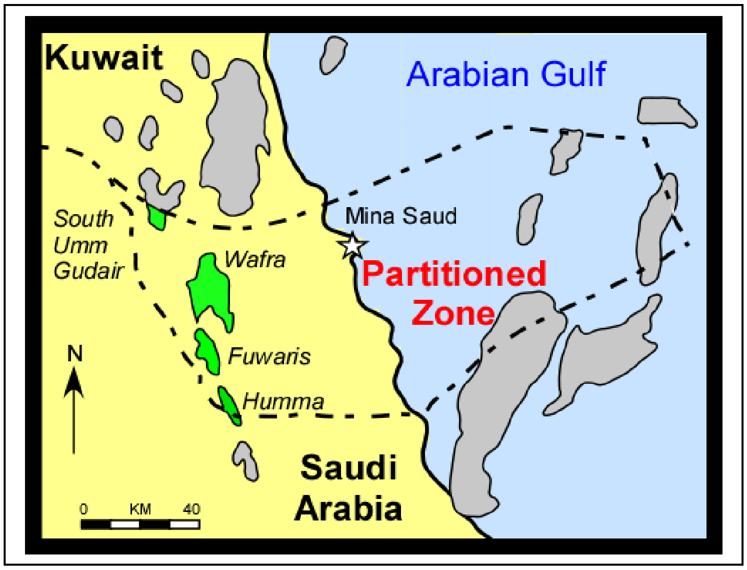


**Figure 1. The Maastrichtian reservoir at Wafra Field is located in the central area of the onshore portion of the Partitioned Neutral Zone (PNZ) between the Kingdom of Saudi Arabia and Kuwait.**

Jennings and Lucia (2003) concluded that rock-fabric classification tends to be more systematically organized within a sequence stratigraphic framework rather than direct use of porosity and permeability data. Similarly, Diaz et al. (2007) applied rock quality index (RQI) and flow zone indicator (FZI) to help quantify rock types and reported successful application on a carbonate reservoir modeling and history match. However, although the rock type (RT) or flow units based methods were reported to improve the classification of the facies from well logs, these methods may have limited predictability in 3D space. This is because rock types or flow units are descriptive concepts, which do not have the same geometry connotation as facies. Instead of direct use of the RT or flow unit curves, these derived curves may improve the performance of neural nets. Using difference or multiplication of inputs may improve the performance of neural nets as noted by Wong et al. (1998).

## Reservoir Description

The Maastrichtian reservoir is located in Wafra field (**Figure 1**, previous page). The Upper Cretaceous-age Maastrichtian reservoir was discovered and first produced in 1959. The reservoir is currently in early development because of its low but variable oil gravity (13-21 ºAPI), high sulfur content, relatively high water-cut, and apparent compartmentalization has made it a much less attractive resource than other productive intervals at Wafra field. Less than 1 percent of the approximately 2-4 billion bbls OOIP in the Maastrichtian has been produced to date.

The Maastrichtian oil production is largely from subtidal dolomites at an average depth of 2500 feet. The average porosity of the reservoir interval is about 15% although productive zones have porosity values up to 30-40%. The average permeability of the reservoir interval is about 30 md. Individual core plugs have measured permeability up to 1200 md. **Figure 2** provides a structure map for the Maastrichtian reservoir at Wafra field. **Figure 3** provides a generalized stratigraphic column for the PNZ.

The Maastrichtian reservoir is mainly composed of dolomite and limestone with thin beds of organic-rich shale. Individual shale layers ranges from less than an inch to several feet. The Second Maastrichtian shale separates the Maastrichtian into an upper and lower portion with significantly different depositional characteristics. The upper portion of the Maastrichtian is also known as the First Maastrichtian reservoir. The lower portion is often referred to as the Second Maastrichtian reservoir. This is shown on the type log in **Figure 4**. The current stratigraphic framework is also summarized in **Figure 4**. Note that this framework was initially established using a small number of wells located mainly along the axis of the structure (**Figure 2**).

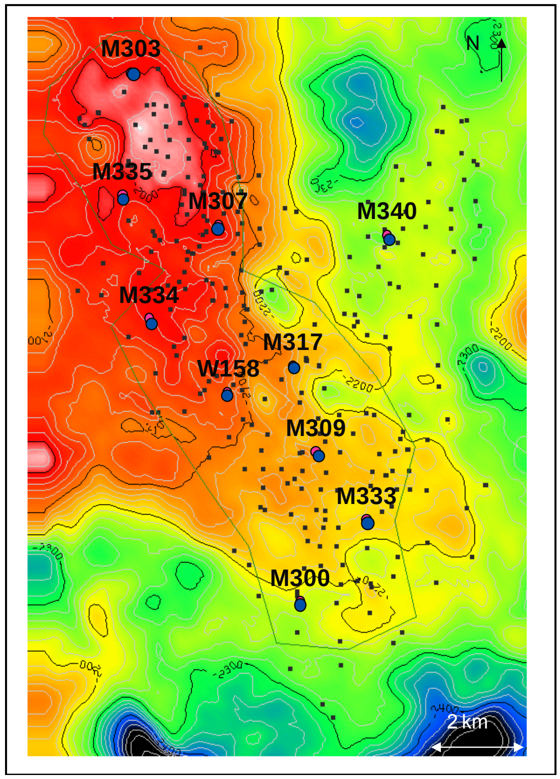


**Figure 2. Structure map for the Wafra Maastrichtian reservoir at Wafra Field, PNZ. Filled blue circles represent cored wells which were used for facies and sedimentary environment interpretation.**

## Input Data

Vendor supplied core descriptions in pdf format were digitized and the vendor's detailed facies classification reduced from 20 or so detailed facies to eight facies for use in this project. The eight facies used in this study were:

1 – Evaporites (mainly anhydrite)
2 – Shale
3 – Mudstone
4 – Wackestone
5 – Floatstone
6 – Mud-rich Packstone
7 – Mud-poor Packstone
8 – Grainstone

Unlike clastic reservoirs, the log responses in carbonate reservoirs are complex and nonlinear (Wong et al., 1998; Dull , 2004). Traditional cutoff methods are usually not adequate to define facies. **Table 1** summaizes the petrophysical properties of the facies listed above for the Maastrichtian reservoir and documents the significant overlap that limits the usefulness of "traditional" statistical approaches for facies classification in carbonate reservoirs.

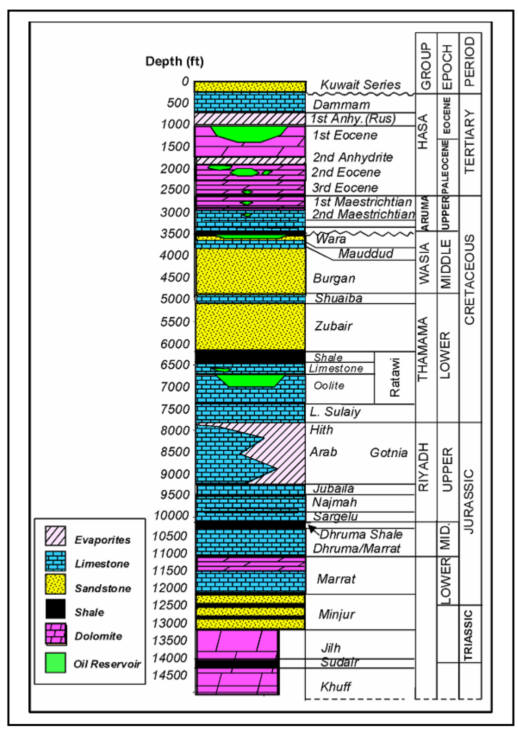


**Figure 3. Generalized stratigraphic column for the PNZ.**

The reduced-facies digital "well log" was integrated with normalized wireline well log data and displayed in a common format for subsequent clean-up. All logs used in this study weree calibrated to remove artifacts from wireline data acquisition. The wireline data was normalized using both the mean and standard deviation of the individual well log curves by stratigraphic unit (e.g. M10, M20, etc; see **Figure 4**). Core to well log depth shifts were reviewed and adjusted if necessary and wireline data outliers removed. Based on previous studies (Wong et al, 1998), the outliers are known to dramatically damage the neural network predictability and need to be removed before the network training. Outliers were defined using the following criteria:

- Intervals with null or missing values
- Intervals with vugs (either from core observation or from significant differences between calculated total porosity and matrix porosity derived from sonic or resistivity logs (Asquith, 1985)
- Intervals with obvious post-depositional overprints (fractures observed in core or image logs)
- Intervals characterized by caliper-indicated wash-outs or bad well bore conditions
- Intervals with acoustic or resistivity well log spikes

The well logs that were used for facies classification included GR, RT, RHOB, NPHI, PE, and RT. The RT log was also included in the training set as the interval used in the study is above the oil water contact..

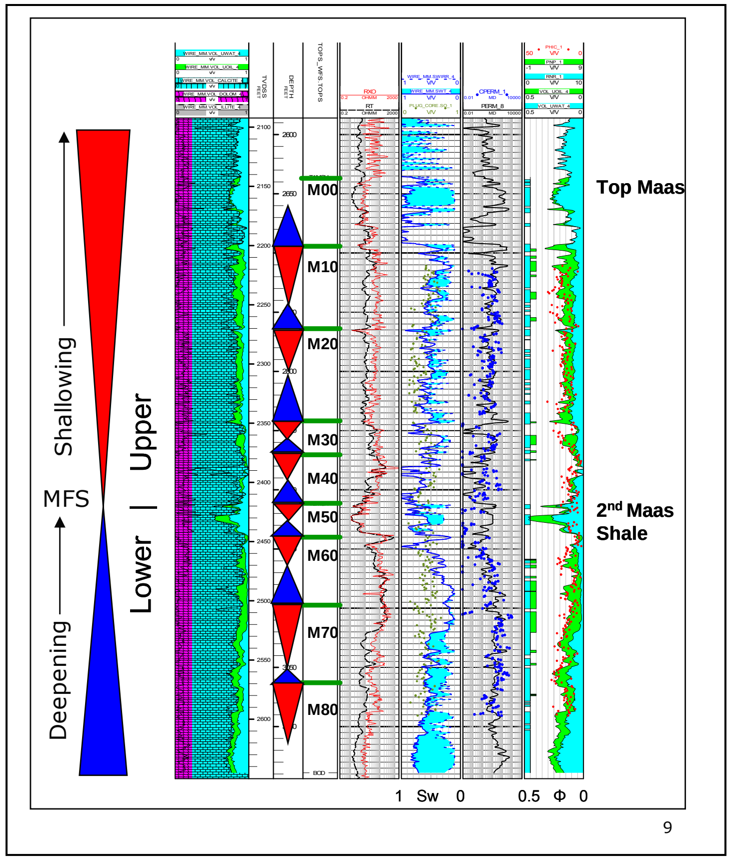


**Figure 4. Type log for the Maastrichtian reservoir showing the current stratigraphic interpretation.**

**Table 1. Overlap of wireline log parameters for the significant facies included in this study. This overlap precludes use of cutoff based methods.**

| | Mudstone | Wackstone | Mudpackstone | GrainPackstone | Floatstone |
|---|---|---|---|---|---|
| Facies Code | 1 | 2 | 3 | 4 | 6 |
| CAL (in) | - | possible wash out | - | - | possible wash out |
| DT (us/ft) | 56-60 | 58-70 | 54-61 | 58-67 | 60-68 |
| GR (API) | 59-75 | 37-67 | 35-71 | 36-71 | 35-93 |
| NPHI (%) | 0.13-0.17 | 0.16-0.23 | 0.13-0.18 | 0.19-0.22 | 0.14-0.22 |
| RHOB (g/cc) | 2.43-2.54 | 2.39-2.61 | 2.45-2.57 | 2.47-2.52 | 2.41-2.58 |
| PE (B/E) | 4.2-4.6 | 2.9-3.3 | 2.9-3.1 | 3.0-4.5 | 2.7-4.1 |
| Porosity | 8-12% | 8-19% | 8-17% | 9-18% | 10-17% |
| Permeability | 0-0.1 md | 1.3-60.3 | 0.1-19 md | 0.4-27 md | 0.4-31 md |

### Facies Prediction Using a Probabilistic Neural Network (PNN)

As mentioned above, facies cannot be classified easily using a cutoff-based methodology due to the overlap of petrophysical response. Several approaches were investigated to see which provide the best results for the Maastrichtian reservoir data. Approaches investigated included multivariate algorithms, discriminant analysis, multivariate logistic regression, beta-bayes method (Tang and Ji, 2006); Tang and White, 2008), and artificial neural network algorithms (such as backward propagation network). The Probabilistic Neural Network (PNN) approach achieved the best results and is described briefly below.

The PNN approach uses a radial basis function (RBF), which is a symmetric Gaussian type function. The RBF is similar to the semivariogram model in kriging, but it does not require the fitting of experimental semivariogram models. The estimator is a linear combination of different RBFs. The weights of linear combinations are estimated using a gradient descent method. The design of the PNN is guaranteed to converge to a Bayesian classifier, providing it is given enough training data. However, it involves more computation steps and thus is slower than other kinds of neural networks used for classification (Mathworks, 2007).

PNN has two layers–the radius basis layer and the competitive layer. The first layer computes distances from input vector to training input vectors. The second layer sums these contributions for each class of inputs to produce a vector of probability. Finally, the most probable group is assigned as the output group. A MATLAB (Mathworks, 2007) code was used to implement the PNN used in this study.

For validation purposes, training sets are randomly selected from each zone from wells M303 and M307. Hold-off data were used to validate prediction ability. The well log data used for facies prediction ultimately included seven logs (GR, SP, DT, NPHI, RHOB, PE, and RT). Some wells have GR spectrum logs, which are better lithological indicators than GR. However, the GR spectrum log is not always run on Maastrichtian wells and was therefore not used in this study. These steps are discussed in more detail below.

### *Optimizing the Spread*

As mentioned above, PNN has two layers – the radius basis layer and the competitive layer. A radial basis function, or RBF, is the distance between weight vector (W) and input vector (V) multiplied by the Bias ($b$). The RBF is expressed:

$$RBF=\mathrm{RadBas}(||W.V||b) \quad (1)$$

Where $\|W.V\|$ is the Euclidian distance between input vector V and weight vector W, which is analogous to distance matrix in discriminant analysis (DA). The bias $\underline{b}$ is similar to a prior in DA. The RBF has a symmetric bell shape distribution. When the input to the RBF is 0, the RBF function has maximum value of 1. As the distance between W and V decreases, the output increases, and vice versa. Thus, the bias $b$ (spread) allows the sensitivity of neurons to be adjusted. "*When the bias or spread = 0, the network will act as a nearest neighbor classifier. As bias becomes larger, the designed network will take into account several nearby vectors*" (Mathworks, 2007). By adjusting the spread b, the PNN will reach the optimum value for a given training set (**Figure 5**). In this study, the spread value of 1 has the best prediction accuracy and is subsequently used for all prediction cases. Furthermore, it is also interesting to notice that M303 has lower prediction accuracy than M307 given the same spread. This may be explained by diagenetic overprints in M303 which complicates log facies responses.

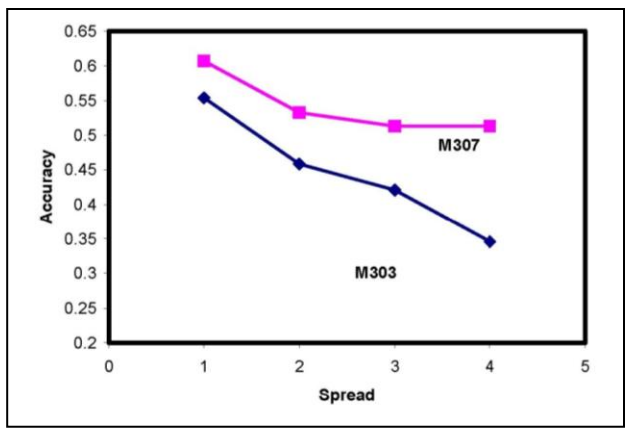


**Figure 5. Change of prediction accuracy vs. spread (bias).**

### *Synthetic Curves*

Several previous facies classification studies have claimed that synthetic logs improve neural network prediction (Wong et al., 1998). Follow the definition of (Lucia, 2005), the Rock Fabric Number (RFN) is generated using following equation (2).

$$\log_{10} RFN = \frac{(3.1107 + 1.8824\log(\phi_t) + \log(S_{wt})}{3.0634 + 1.4045\log(\phi_t)} \quad (2)$$

In which $\phi_t$ and $S_{wt}$ are total porosity and total water saturation. This empirical equation of RFN needs to be used above the water oil contact.

Similarly, the rock quality index (RQI) and flow zone index (FZI) proposed by (Diaz et al., 2007) is given by

$$RQI = 0.0314\sqrt{\frac{K}{\phi_t}} \tag{3}$$

in which $K$ is the permeability and $\phi_t$ is the total porosity. Diaz et al. (2007) used the permeability and porosity to define rock types from core and a linear regression method to predict FZI, and RQI in well bores. In this study, the inclusion of these synthetic logs did improve the prediction accuracy.

## Validation and Application

### *Effects of Sample Size*

Including more samples into the neural network increases the prediction accuracy (Tang and White, 2008). This is illustrated in **Figure 6** which visually shows the improved match between predicted facies and described facies for one of the Maastrichtian wells. With increasing fraction of input data used for the training set, the predicted facies becomes more similar to the core description. **Figure 7** shows the overall prediction accuracy increases from 63% (using 25% of the available data as input) to 85% (using 75% of the data as input) in M303. For well M307 an increase in accuracy from 73% to 89% is obtained by similarly increasing the sample size. PNN is a robust predictor. The difference in prediction accuracy obtained from well M307 and well M303 may reflect differences in post-depositional overprint at these two locations.

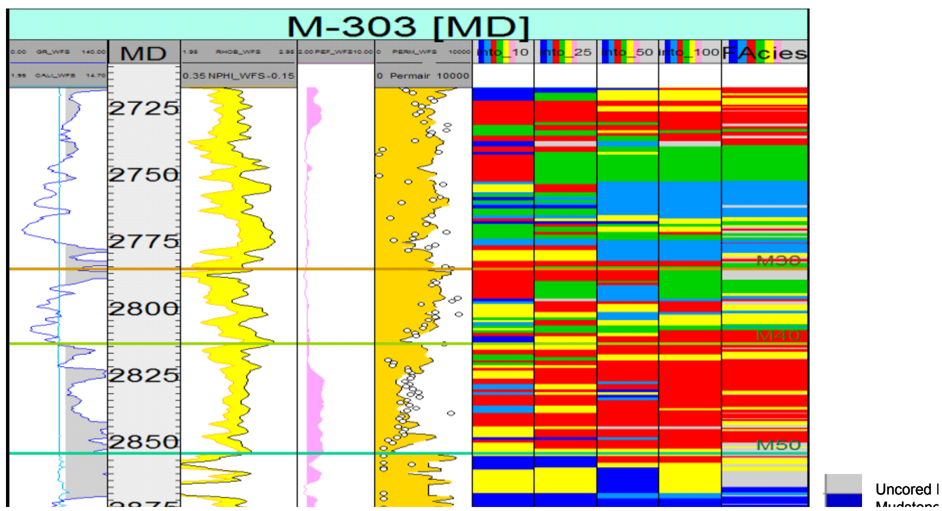


**Figure 6. With increasing fraction of iut data used for the training set (10% to 100%), the predicted facies is becomes more similar to the core description (far right column).**

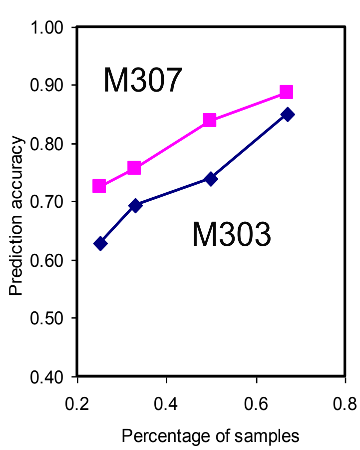


**Figure 7. Plot showing increase in prediction accuracy as the fraction of input data used for training increases from 20% to 70%. The difference in prediction accuracy between the two wells, M307 and M303, may reflect differences in post-depositional effects such as diagenesis.**

### *Effects of Well Log Inputs*

Tang and White (2008) concluded that including more logs will also increase prediction accuracy. This is shown for the Maastrichtian reservoir data in **Figure 8**. Note that the prediction accuracy gradually increases from about 48% to 69% as more well log types are included. Note also that in this analysis only 12.5% of the input data is used for training the PNN. It is also interesting to note that including different log will increase the accuracy to different extents. For example, by including GR and NPHI, the accuracy shows significant improvement; however, including DT log does not significantly improve the accuracy. This is likely explained by the fact that different logs will add different levels of "new" information to the neural net. As a result, new independent information will significantly increase the identification ability; while, redundant or even conflicting information would reduce the identification ability. For large sets of log data, principle component analysis (PCA) could be used to increase the computational efficiency by removing the redundant information.

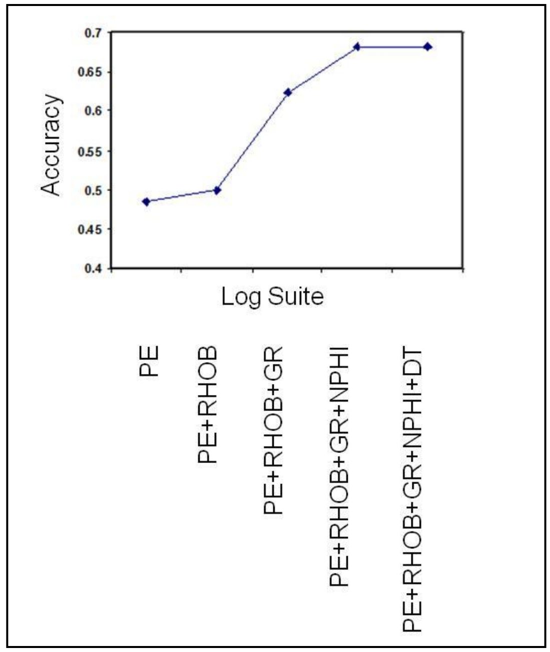


**Figure 8. Impact of increasing the number of well log curves used for classification.**

### *Effect of Adding Synthetic Curves*

Including the synthetic curves RQI and RFN (described above) significantly improves facies prediction. Note that without the synthetic curves, the prediction accuracy is less than 50% for individual facies If the synthetic curves are included, the prediction accuracy by facies type ranges from about 55% to over 70% as shown in **Table 2**. Note that the input sample sets used to construct the two parts of **Table 2** was slightly different.

### *Cross Validation using Hold-Off Data*

In cross validation part of the core data is used as training input and part is held off for validation purpose. **Table 3** shows the cross validation results for well M307. In this test 25% of the M307 well data was used as input for training. Note that most samples are correctly classified. Prediction accuracy by facies type ranges from ~55% to over 85%. Cross validation against a hold off well (blind test) is shown in **Figure 9**. The PNN was trained using data from well M309 and used to predict facies in well M300. The cross validation matrix (**Table 3**) shows 54-73% prediction accuracy for common facies and significantly lower accuracy for less common facies.

|  | 1 | 2 | 3 | 4 | 5 | 6 |  |
|---|---|---|---|---|---|---|---|
| 1 | **0** | 0 | 14 | 19 | 0 | 6 | 39 |
|  | 0.00% | 0.00% | 35.90% | 48.72% | 0.00% | 15.38% | 100.00% |
| 2 | 0 | **0** | 150 | 69 | 39 | 0 | 258 |
|  | 0.0% | 0.0% | 58.1% | 26.7% | 15.1% | 0.0% | 100.0% |
| 3 | 0 | 0 | **81** | 17 | 79 | 0 | 177 |
|  | 0.0% | 0.0% | 45.8% | 9.6% | 44.6% | 0.0% | 100.0% |
| 4 | 0 | 0 | 30 | **25** | 6 | 46 | 61 |
|  | 0.0% | 0.0% | 49.2% | 41.0% | 9.8% | 75.4% | 100.0% |
| 5 | 0 | 0 | 0 | 0 | **0** | 0 | 0 |
|  | 0.0% | 0.0% | 0.0% | 0.0% | 0.0% | 0.0% | 0% |
| 6 | 0 | 6 | 46 | 74 | 0 | **95** | 221 |
|  | 0.0% | 2.7% | 20.8% | 33.5% | 0.0% | 43.0% | 100.0% |
| Total | 0 | 6 | 321 | 204 | 124 | 147 | 802 |
|  | 0.0% | 0.7% | 40.0% | 25.4% | 15.5% | 18.3% | 100.0% |

|  | 1 | 2 | 3 | 4 | 5 | 6 |  |
|---|---|---|---|---|---|---|---|
| 1 | **1** | 0 | 18 | 20 | 0 | 0 | 39 |
|  | 2.56% | 0.00% | 46.15% | 51.28% | 0.00% | 0.00% | 100.00% |
| 2 | 1 | **29** | 59 | 48 | 4 | 117 | 141 |
|  | 0.7% | 20.6% | 41.8% | 34.0% | 2.8% | 83.0% | 100.0% |
| 3 | 30 | 5 | **79** | 33 | 1 | 29 | 148 |
|  | 20.3% | 3.4% | 53.4% | 22.3% | 0.7% | 19.6% | 100.0% |
| 4 | 4 | 2 | 26 | **42** | 0 | 33 | 74 |
|  | 5.4% | 2.7% | 35.1% | 56.8% | 0.0% | 44.6% | 100.0% |
| 5 | 0 | 0 | 0 | 0 | **0** | 0 | 0 |
|  | 0.0% | 0.0% | 0.0% | 0.0% | 0.0% | 0.0% | 0% |
| 6 | 2 | 3 | 43 | 12 | 0 | **161** | 221 |
|  | 0.9% | 1.4% | 19.5% | 5.4% | 0.0% | 72.9% | 100.0% |
| Total | 38 | 39 | 225 | 155 | 5 | 340 | 802 |
|  | 4.7% | 4.9% | 28.1% | 19.3% | 0.6% | 42.4% | 100.0% |

**Table 2. The top table gives the initial prediction results for blind well test using well M300 based on training using well M309 without synthetic curves. The bottom table shows increased accuracy of predictions when the two synthetic curves, RQI and RFN, are included in the training and prediction.**

### *Uncertainty Estimation*

One advantage of using probabilistic neural networks is the prediction uncertainty could be quantified by probability logs. Probability logs used in this study were generated by scaling input vectors. Each output has a "tendency" to be classified as one of the facies categories defined when the network is created. We use this tendency to find the probability that a certain input will result in a certain classification category. This is done by looking at the input to the compete function in the PNN network. The input vector of the compete function is then scaled by the summation of the vectors and has a range of between 0 and 1. The resulting scaled input vector of compete is used as a “probability”.

Because the “probability” is generated by scaling input vectors of a transfer function, there is a chance of being “overly optimistic” in the prediction. For instance, if there are data that do not lie exactly between the categories which were used to train the network, the network will create a probability for a single category of 1. To quantify the uncertainty of facies prediction, two logs are generated from the vector of the probabilistic logs, the so-called confidence and discriminant ability logs. The confidence log is the probability associated with the most likely facies; and the discriminant ability log is the confidence minus the probability of the second most likely facies. The confidence log indicates how confident the prediction is and discriminant ability illustrates how much the predicted facies different from other facies. Tang and Ji (2006) described the details of the facies uncertainty statistics. **Figure 9** illustrates the predicted facies for well M307. The predicted facies is plotted to compare with the core facies. The predicted facies shows more “detail”, which represents the high frequency variation of log values. The two uncertainty logs are plotted so that the enclosed area represents the uncertainty of prediction. If the enclosed area is 0, it means the prediction is certain; or the log data combination at given depth is similar to the facies from training sets. Otherwise, the prediction is not certain. However, as mentioned above the PNN derived “probability” tends to be optimistic. Caution should be exercised when using the uncertainty logs for interpretation.

| | | Predicted Facies | | | | |
|---|---|---|---|---|---|---|
| | | 2 | 3 | 4 | 6 | Accuracy |
| Geological Prior Facies | 2 | **60** | 12 | 12 | 8 | 92 |
| | | **65.2%** | 13.0% | 13.0% | 8.7% | 100.0% |
| | 3 | 5 | **13** | 3 | 3 | 24 |
| | | 20.8% | **54.2%** | 12.5% | 12.5% | 100% |
| | 4 | 6 | 6 | **28** | 4 | 44 |
| | | 13.6% | 13.6% | **63.6%** | 9.1% | 100% |
| | 6 | 2 | 5 | 5 | **100** | 112 |
| | | 1.8% | 4.5% | 4.5% | **89.3%** | 100% |
| | Total | 73 | 36 | 48 | 115 | 272 |
| | Accuracy | 26.8% | 13.2% | 17.6% | 42.3% | **74%** |

(Used 25% of sample as training set)

**Table 3. Cross validation results for well M307. In this test 25% of the M307 well data was used as input for training. Note that most samples are correctly classified. In addition to well log curves, the two synthetic curves were also included in the PNN training set.**

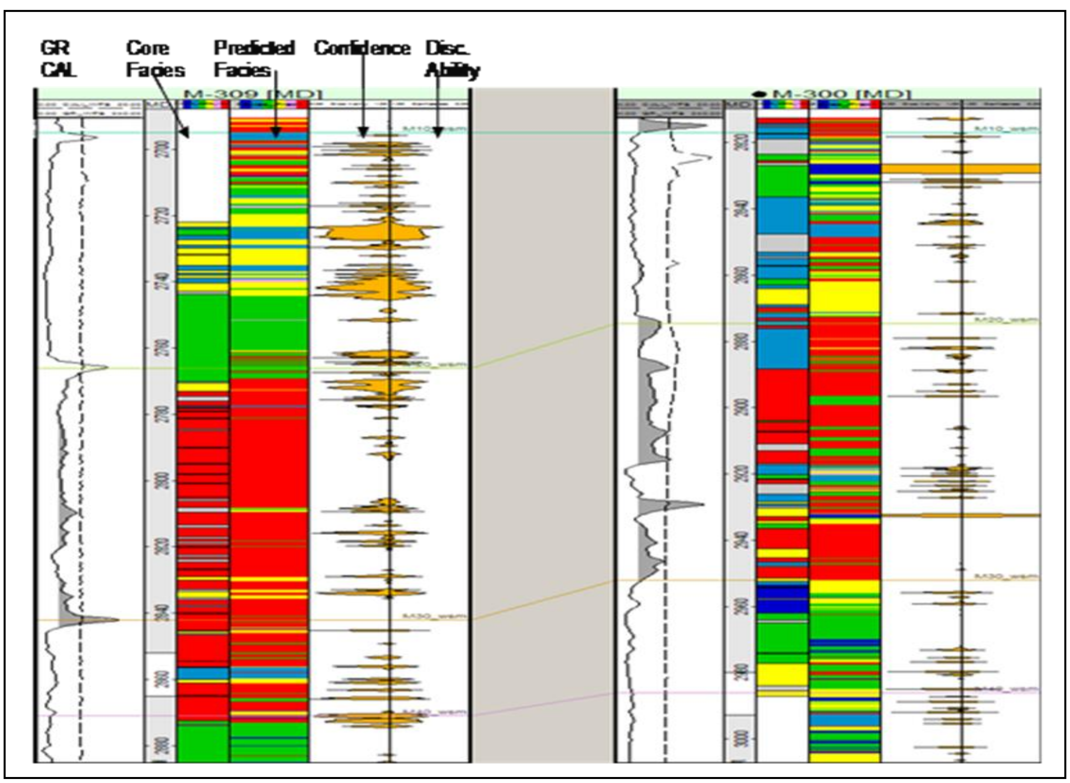


**Figure 9. Visual comparison of prediction accuracy for blind well test. Numerical results of the hold off well cross validation (blind well test) are given below. Probability curves (Confidence and Discriminant Ability are described below.**

*Application in Stratigraphic and Sedimentary Interpretation*

The predicted facies logs for the 15 selected key wells has been successfully applied by Toomey et al (2009) to improve the stratigraphic framework for the reservoir (**Figure 10**). The additional facies logs for flank wells also add useful information for depositional interpretation. **Figure 11** shows the change of sedimentary environment interpretation based on the additional well log data compared to the original interpretation based on the available six cored and described wells. The original zones of sedimentary environment are preserved, however, additional facies logs improve the boundary location of these zones. These results will impact future decisions on infill drilling as well as additional data acquisition including cored wells.

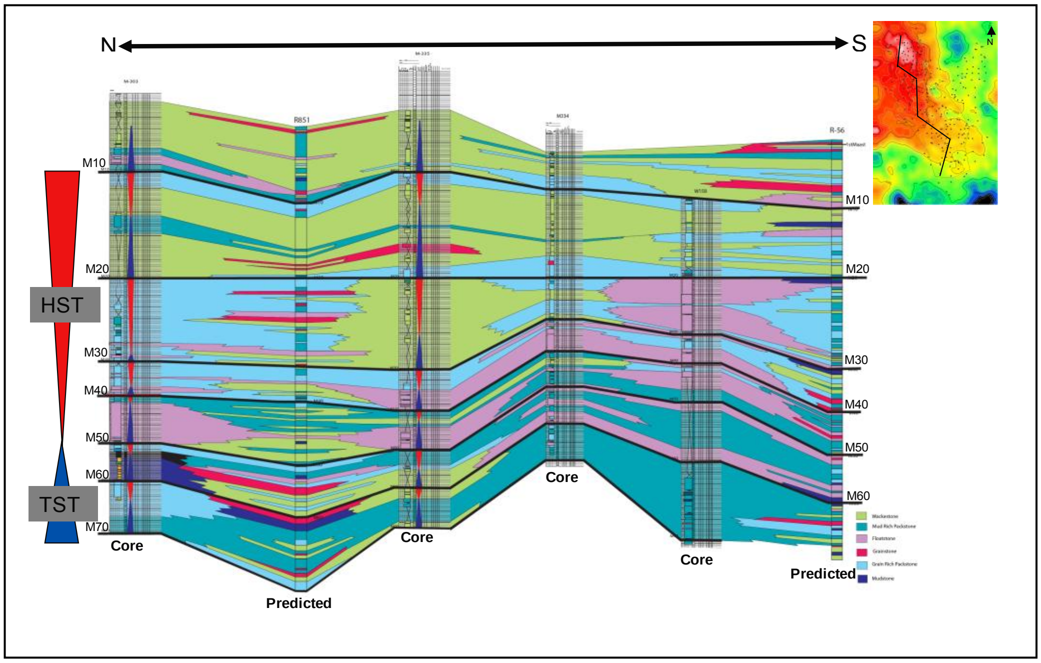


**Figure 10. Interpreted stratigraphic cross section (Toomey et al, 2009) showing impact of facies predictions obtained using the PNN workflow.**

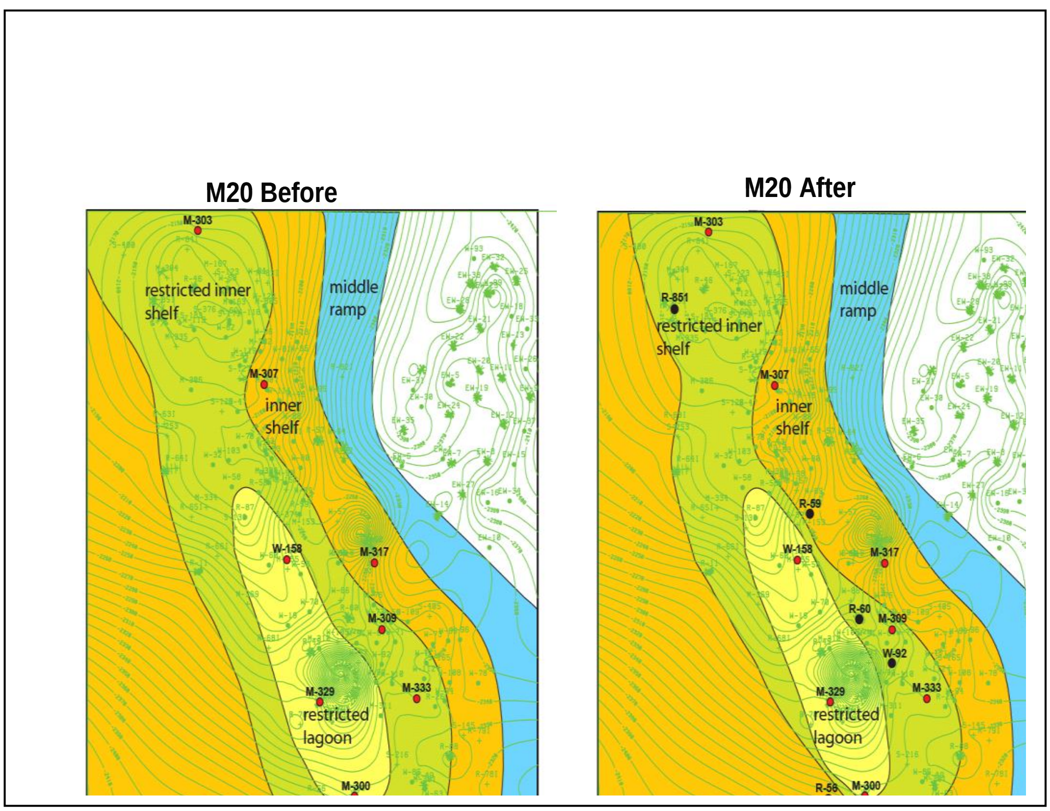


**Figure 11. Change of sedimentary environment interpretation for the M20 stratigraphic interval based on the cored and predicted facies in key, un-cored wells as compared to maps generated using only the originally available six cored and described wells (Toomey et al, 2009). Red circles are original cored wells. Black circles are new wells with log derived facies.**

## Limitations

The reliability of the neural net prediction strongly depends on the input provided by training data. To ensure an accurate prediction, adequate training data are needed. However, more data does not always result in better prediction. Acquiring representative training samples and remove outliers based on geological knowledge is critical for quality control. Current PNN cannot recognize spatial pattern, even. As a result, the gradual change in log responses results in high frequency variation in facies prediction. To remove the artifacts, geological knowledge should be used to post-process the predictions. PNN builds patterns based on existing data; it cannot predict facies that do not exist in the training data. The PNN predicted facies should be used as a soft guidance instead of as hard facies curve. Based on the results of this study, the workflow was used to predict facies for 15 key wells in the Maastrichtian reservoir at Wafra Field.

## Acknowledgements

The authors thank Chevron for permission to publish this paper. We also thank Mr. Dennis Dull and Dr. Bobby Kurnianwan for providing constructive suggestions on general carbonate facies modeling and data input/output using GEOLOG.

## References

Ameen, M. S., Hailwood, E. A., 2008. A new technology for the characterization of microfractured reservoirs (test case: Unayzah reservoir, Wudayhi Field, Saudi Arabia). AAPG Bulletin 92 (1), 31–52.

Asquith, G. B., 1985. Handbook *of Log Evaluation Techniques for Carbonate Reservoirs*, AAPG Methods in Exploration Series, 5th Edition.

Dehghani, K., Harris, P. M. M., Edwards, K. A., Dees, W. T., 1999. Modeling a vuggy carbonate reservoir, McElroy Field, west Texas. AAPG Bulletin 83 (1), 19–42.

Diaz, G. G. M. A., Paz, F., Smalley, J., Waninger, E. A., 2007. Rock typing as an effective tool for permeability and water-saturation modeling: A case study in a clastic reservoir in the Oriente Basin (SPE-97033). SPE Reservoir Evaluation and Engineering 10 (6), 730–739.

Dull, D. W., 2004. Integrating sequence stratigraphy and multiple three-dimensional geostatistical realizations in constructing a model of the Second Eocene reservoir, Partitioned Neutral Zone, Wafra Field, Kuwait and Saudi Arabia. *Integration of Outcrop and Modern Analogs in Reservoir Modeling*, AAPG Memoir 50/SEPM Special Publication, 309–336.

Dull, D. W., Garber, R. A., Meddaugh, W. S., 2001. Maastrichtian Reservoir Characterization, ChevronTexaco internal report, 50 p.

Dull, D. W., Garber, R. A., Meddaugh, W. S., 2006. The sequence stratigraphy of the Maastrichtian (Upper Cretaceous) reservoir at Wafra Field, Partitioned Neutral Zone, Saudi Arabia and Kuwait: Key to reservoir modeling and assessment. *Giant Hydrocarbon Reservoirs of the World: From Rocks to Reservoir Characterization and Modeling*, AAPG Memoir 88/SEPM Special Publication, 247–279.

Holtz, M. H., Major, R., 2004. Integrated geological and petrophysical characterization of Permian shallow-water dolostone (SPE-87595). SPE Reservoir Evaluation and Engineering 7 (1), 47–58.

Jennings, J. W., Lucia, F. J., 2003. Predicting permeability from well logs in carbonates with a link to geology for interwell permeability mapping (SPE-84942). SPE Reservoir Evaluation and Engineering 6 (4), 215–225.

Lee, S., Kharghoria, A., Datta-Gupta, A., 2004. Electrofacies characterization and permeabil-ity predictions in complex reservoirs. Society of Petroleum Engineers (SPE-88476). Reservoir Evaluation and Engineering, 237–248.

Lim, J.-S., Kang, J. M., Kim, J., 1997. Multivariate statistical analysis for automatic electro-facies determination from well log measurements (SPE-38028). SPE Asia Pacific Oil and Gas Conference and Exhibition, 14-16 April 1997, Kuala Lumpur, Malaysia.

Lim, J.-S., Kim, J., 2004. Reservoir porosity and permeability estimation from well logs using fuzzy logic and neural networks (SPE-88476). SPE Asia Pacific Oil and Gas Conference and Exhibition, 18-20 October 2004, Perth, Australia.

Lucia, J. F., 2005. *Carbonate Reservoir Characterization*, 2nd Edition. Springer-Verlag, New York.

Mathisen, T., Lee, S. H., Datta-Gupta, A., 2003. Improved permeability estimates in carbonate reservoirs using electrofacies characterization: A case study of the North Robertson Unit, west Texas (SPE-84920). SPE Reservoir Evaluation and

Engineering 6 (3), 176–184.

Mathworks, I., 2007. Neural Network Toolbox User's Guide for use with MATLAB, Chapter 6. MathWorks, Inc.

Qi, L. S., Carr, T. R., 2006. Neural network prediction of carbonate lithofacies from well logs, Big Bow and Sand Arroyo Creek fields, southwest Kansas. Computers and Geosciences 32, 947–964.

Tang, H., Ji, H., 2006. Incorporation of spatial characters into volcanic facies and favorable reservoir prediction (SPE–90847). SPE Reservoir Evaluation and Engineering 9 (5), 565–573.

Tang, H., White, C. D., 2008. Multivariate statistical log log-facies classification on a shallow marine reservoir. Journal of Petroleum Science and Engineering, doi:10.1016/j.petrol.2008.05.004.

Toomey, N., Tang, H., and Meddaugh , W. S., 2009. Using Neural Network Predicted Facies to Refine the Stratigraphic Framework; Maastrichtian Reservoir at Wafra Field, Partitioned Neutral Zone (PNZ), Saudi Arabia and Kuwait, AAPG Denver Meeting, June 2009 (abstract).

Wong, P. M., Henderson, D., Brooks, L., 1998. Permeability determination using neural networks in the Ravva Field, offshore India. Reservoir Evaluation and Engineering, 99–104.